Characterization of yellow pyrazolyl azo pigments with or without Na integrated as the central metal

Hiroki Shibata and Jin Mizuguchi; Department of Applied Physics, Yokohama National University; Yokohama, Kanagawa/Japan

Abstract

We were so far involved in the X-ray structure analysis of the title compounds in order to improve their solvent fastness from the structural point of view. Unexpectedly, we have isolated, from the same reaction pot, three kinds of single crystals: two Na-containing bisazo compounds of the cis form and one Na-free monoazo one. In addition, a Na-free bisazo compound of the trans form has also been isolated by eliminating the Na atom of the former by means of HCl. In the present investigation, we have carried out the electronic characterization of the Na-free bisazo compound together with its light-, heat-, and solvent fastness. As a result, the Na-free bisazo compound is found to exhibit a vivid yellow and possess a high fastness against light, heat and organic solvents.

1. Introduction

As is well known, azo pigments are widely used in imaging and printing industries because of their versatile colors, high tinctorial strength as well as their low price [1]. However, the azo pigments are generally inferior in light-, heat-, and solvent fastness to phthalocyanines (blue), peryleneimides (vivid red *via* maroon to black), quinacridones (red and magenta), pyrrolopyrroles (red), although considerable effort has been directed to improve these properties. Under these circumstances, some novel azo pigments with high light- and heat-stability (but poor solvent fastness) have recently been reported by Nagata *et al*. which include 2,6-bis[5-amino-3-*tert*-butyl-4-(3-methyl-1,2,4-thiadizol-5-yldiazeneyl)-1*H*-pyrazol-1-yl]-1,3,5-triazin-4(1*H*)-one (B-PAT: Fig. 1) [2]. In our previous investigation [3], we have carried out structure analysis of B-PAT in order to improve the solvent fastness from a structural point of view. Unexpectedly, we have isolated three kinds of single crystals from the reaction product of B-PAT, indicating that the product was not a pure material, but a mixture of mono and bisazo compounds. To our even greater surprise, the bisazo compounds are found to form five-coordinate Na-complexes in a *cis* fashion (Na-containing B-PAT [4, 5]: about 80 % of the product; Fig. 2 (a)); whereas the monoazo compound is Na-free (M-PAT [6]: about 20 % : Fig. 2 (b)). We wondered why the Na atom is included in B-PAT and why the Na-complex crystallizes in a *cis* fashion, because the *cis* form is generally less stable than the *trans* one. Then, we found that $NaNO_2$ used for the preparation of diazo components is responsible for the Na inclusion and that the Na atom bridges by force two monoazo moieties in a *cis* fashion. In addition, the inclusion of the Na-atom in B-PAT greatly stabilizes B-PAT as compared with B-PAT of the *cis* or *trans* form according to our molecular orbital calculations. This prompted us to eliminate the Na atom from Na-containing B-PAT in an attempt to obtain another B-PAT of the *trans* form (Fig. 1(b)) that might exhibit high solvent fastness. In fact, we could isolate Na-free B-PAT of the *trans* form by addition of hydrochloric acid [3]. Then, Na-free B-PAT of the *trans* form is found to possess high solvent fastness in addition to the light- and heat-stability of the original title compound.

The present paper reports on the electronic structure as well as on the light-, heat- and solvent fastness of the Na-free B-PAT of the *trans* form, using the originally synthesized product (*i.e.* mixture of Na-containing B-PAT and M-PAT) as the reference.

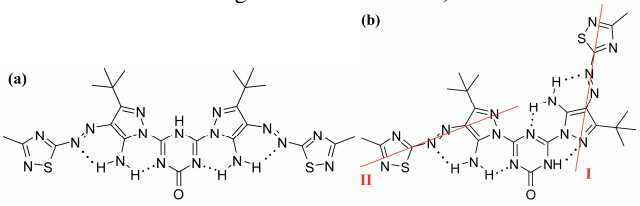

Fig. 1 Structure of B-PAT: (a) cis form and (b) trans form. The solid lines designate the direction of the transition dipole.

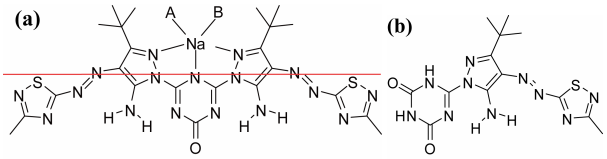

Fig. 2 Structure of three isolated crystals: (a) Na-containing B-PATs (B-PAT I with A = methanol and B = phenol: B-PAT II with A = water and B = NMP) and (b) Na-free M-PAT. The solid line denotes the direction of the transition dipole according to the molecular orbital calculations [3].

2. Experimental

2.1. Preparation of B-PAT and Na-free B-PAT

The mixture of mono and bisazo compounds (*i.e.* intended B-PAT: Fig. 1) was synthesized as described in a previous report [2]. The ratio of the mono to bisazo compounds is estimated to be about 1 to 4 on the basis of the elementary analysis.

Na-free B-PAT was immediately precipitated from a B-PAT-saturated solution in NMP upon dissolution of HCl with 30 times molar equivalent. The product was isolated by filtration and washed with water. Elementary analysis gave the formula of $C_{23}H_{29}N_{17}OS_2 \cdot H_2O$ which is in good agreement with the theoretical value of B-PAT being non-water (M_w: $C_{23}H_{29}N_{17}OS_2$ = 623.72). In addition, mass spectrum gave the parent peak of 624 for B-PAT together with some small fractions, as shown in Fig. 3.

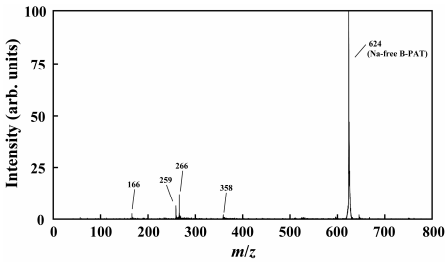

Fig. 3 Mass spectrum of Na-free B-PAT of the trans form.

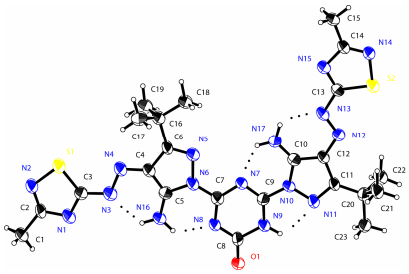

Fig. 4 ORTEP plot for Na-free B-PAT of the trans form.

2.2. Spectroscopic calculations on Na-free B-PAT of the trans form

Semi-empirical molecular orbital (MO) calculations were carried out on Na-free B-PAT of the *trans* form, using MOPAC2009. Geometry was optimized with the AM1 Hamiltonian, and the spectroscopic calculations were made on the optimized geometry using ZINDO method.

2.3. Summary of the structure of Na-containing B-PAT, Na-free B-PAT, and M-PAT

Table 1 summarizes the crystallographic parameters for Na-containing B-PATs I and II of the *cis* form [4, 5], Na-free B-PAT of the *trans* form, and Na-free M-PAT [6]. Na-containing B-PAT I of the *cis* form is the five-coordinate Na-complex with A = methanol and B = phenol, while B-PAT II designates the similar complex with A = water and B = NMP, as shown in Fig. 2 (a). Only Na-free B-PAT of the *trans* form is free from solvents, and all the rest is solvated crystals.

Fig. 4 shows the *ORTEP* plot of Na-free B-PAT of the *trans* form. The *trans* form is more stable than the *cis* one in the absence of the Na atom according to the MO calculations [3]. There are five NH···N intramolecular hydrogen bonds formed between the NH of the amino group of the pyrazol ring and the N atom of the azo bond.

Fig. 5 illustrates the in-plane dimer structure formed by two NH···O intermolecular hydrogen bonds. The formation of dimers doubles the molecular unit to significantly stabilize the solid state. The molecules are stacked with little molecular overlap, as shown in Fig. 6.

The powder X-ray simulation based on the present structure analysis is in good agreement with the experimental result of Na-free B-PAT of the *trans* form, indicating that the phase of single crystals is identified as the same as that of the powders.

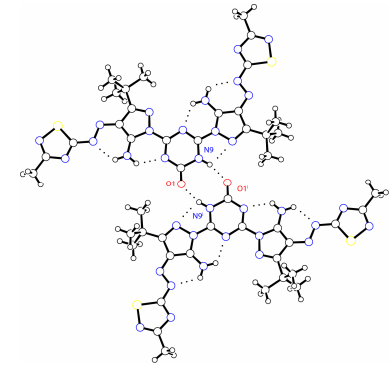

Fig. 5 Dimeric structure of Na-free B-PAT of the trans form. [symmetry code(i): (1-x, 2-y, 1-z)]

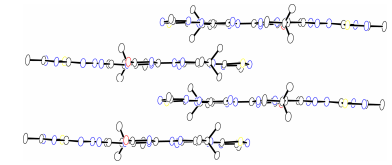

Fig. 6 Molecular stack of Na-free B-PAT of the trans form.

Table 1 Crystallographic parameters.

	Na-containing B-PAT I of the *cis* form	Na-containing B-PAT II of the *cis* form	Na-free B-PAT of the *trans* form	M-PAT
Molecular formula	$C_{50}H_{38}N_{17}O_5S_2Na$ ·4(C_6H_6O)	$C_{28}H_{39}N_{18}O_3S_2Na$ ·C_5H_9NO	$C_{23}H_{29}N_{17}OS_2$	$C_{13}H_{16}N_{10}O_2S$ ·C_5H_9NO·H_2O
Molecular weight	1148.3	861.98	623.72	493.54
Crystal system	triclinic	triclinic	triclinic	monoclinic
Space group	*P*-1	*P*-1	*P*-1	*C*2/*c*
Z	2	2	2	8
a (Å)	8.38964(15)	12.1100(8)	6.7561(12)	27.8283(5)
b (Å)	18.8780(3)	13.7781(9)	14.054(2)	7.02690(10)
c (Å)	20.4060(4)	14.6695(9)	16.203(3)	26.4417(4)
α (°)	114.1030(7)	63.125(3)	83.924(6)	-
β (°)	96.5800(8)	89.298(3)	83.276(7)	91.3430(7)
γ (°)	95.6500(8)	73.534(3)	79.140(7)	-
V (Å^3)	2892.83(9)	2074.4(2)	1495.0(4)	4582.69(13)
D_X (g/cm^3)	1.318	1.38	1.385	1.431
R_1	0.0726	0.1478	0.1373	0.0493

2.4. Measurements of solution and solid-state spectra

UV-visible absorption spectra in solution and in evaporated films were recorded on a UV-2400PC spectrophotometer (Shimazu). Diffuse-reflectance spectra for powders were measured on the same spectrophotometer in combination with an integrating sphere attachment (ISR-240 from Shimazu). Reflection spectra on single crystal were measured by means of a UMSP80 microscope-spectrophotometer (Carl Zeiss). An Ultrafluar (×10) objective was used together with a Nicol-type polarizer. Reflectivities were corrected relative to the reflection standard of silicon carbide.

2.5. Light-, heat-, and solvent fastness of Na-free B-PAT of trans form

Light stability was tested by exposing powdered Na-free B-PAT of *trans* form to UV light directly under a 250W ultrahigh pressure mercury lamp (USHIO) for 10 h. Diffuse-reflectance spectra were measured every one hour in order to study the deterioration of the substance. Thermogravimetric analysis (TGA) was carried out in air for powdered Na-free B-PAT, using Thermo

Plus TG-8120 from Rigaku. Solubility was measured in DMA (dimethylacetoamide) and NMP (*N*-methyl-2-pyrrolidone).

3. Results and discussion

3.1. Electronic structure

3.1.1. Spectroscopic calculations

MO calculations revealed that there are two optical absorption bands in the visible region around 415 and 403 nm. The former transition with an oscillator strength of 1.08 is composed of three main components: HOMO (highest occupied molecular orbital) to LUMO (lowest unoccupied molecular orbital)+1, HOMO to LUMO+2, and HOMO-1 to LUMO. This gives the direction of transition dipole I as shown in Fig. 1(b). On the other hand, the latter transition with an oscillator strength of 0.34 comprises the transitions of HOMO-1 to LUMO and HOMO to LUMO+1. This transition corresponds to the direction of transition dipole II.

3.1.2. Solution spectra

Fig. 7 shows the solution spectrum of Na-free B-PAT of *tarns* form in NMP. The spectrum exhibits a broad band between 380 and 500 nm, which is indicative of a series of vibronic transitions. These are assigned to the 0-0 (pure electronic transition) at the longest wavelength, then the 0-1 and 0-2 transition as shown, assuming that the main transition is due to transition dipole I and that a vibrational transition of about 1800 cm^{-1} is coupled with the pure electronic transition. The absorption maximum at about 450 nm is assigned to the 0-1 transition as characterized by a high extinction coefficient of about 40000.

No significant difference is observed between the spectra of Na-free B-PAT of the *trans* form and the mixture of Na-containing B-PAT of the *cis* form and M-PAT.

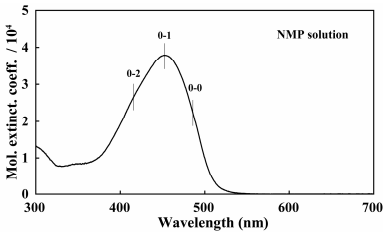

Fig. 7 Solution spectrum of Na-free B-PAT of the trans form in NMP.

3.1.3. Solid-state spectra

Fig. 8 shows the diffuse reflectance spectra for powders of Na-free B-PAT of the *trans* form, together with the absorption spectrum of evaporated films. The spectrum of evaporated films appreciably resembles that in solution (Fig. 7). On the other hand, the diffuse reflectance spectrum is broader than that of the evaporated film. In addition, the absorption maximum appears at about 420 nm and is located slightly at shorter wavelengths than that of the evaporated film, indicating the absorption maximum is now attributed to the 0-2 transition. The evaporated film of Na-free B-PAT exhibits typical yellow, while the powdered Na-free B-PAT is slightly reddish.

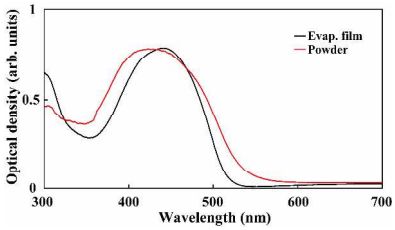

Fig. 8 Diffuse-reflectance and absorption spectra of powdered and evaporated Na-free B-PAT of the trans form, respectively

Fig. 9 shows the non-polarized reflection spectra of Na-free B-PAT of the *trans* form measured on single crystals by means of a microscope spectrophotometer. The reflection spectrum looks similar to that of the diffusion reflectance spectrum (Fig. 8), peaking at 420 nm. Since there are two optical transitions in the visible region (see section 3.1.1) and the situation is rather complicated, we are not yet in the position to precisely characterize the reflection bands by polarization experiments on single crystals.

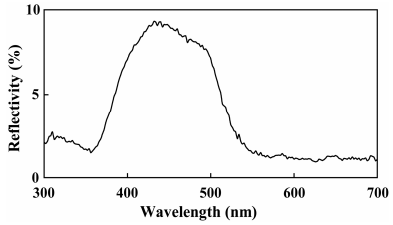

Fig. 9 Non-polarized reflection spectra measured on single crystals of Na-free B-PAT of the trans form.

The situation is slightly different in single crystals of Na-containing B-PAT II of the *cis* form (Table 1) where there is only one optical transition whose transition dipole is shown in Fig. 2. Fig. 10 shows the polarized reflection spectra of Na-containing B-PAT II of the *cis* form. An intense reflection band appears around 500 nm for polarization perpendicular to the *a* axis (*i.e.* the direction of the transition dipole). Polarization parallel to the *a* axis quenches entirely the reflection, indicating that the transition dipole points along the long molecular axis (*i.e.* perpendicular to the *a* axis.). The longest-wavelength band is assigned to the 0-0 transition.

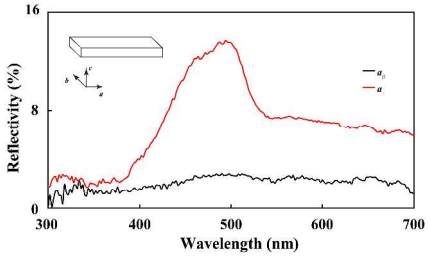

Fig. 10 Polarized reflection spectra measured on the (a, b) plane of Na-containing B-PAT II single crystals.

3.2. Light-, heat-, and solvent fastness

3.2.1. Light stability

Fig. 11 shows the diffuse-reflectance spectra of powdered Na-free B-PAT of the *trans* form before and after UV exposure. No noticeable deterioration is observed after exposure for 10 h, showing a high stability of Na-free B-PAT of *trans* form.

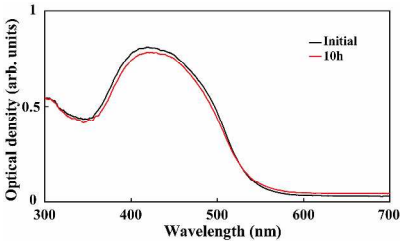

Fig. 11 Diffuse-reflectance spectra of Na-free B-PAT before and after UV exposure.

3.2.2. Heat stability

Fig. 12 shows the TGA curve as a function of temperature for powdered Na-free B-PAT of *trans* form. At first, the weight-loss of about 3 % is observed in the temperature range between 50 and 250 °C. This is due to the desorption of one water molecule adsorbed on the surface of Na-free B-PAT of *trans* form, as pointed out also in elementary analysis (see section 2.1). The weight-loss begins to occur abruptly around 340 °C, indicating that Na-free B-PAT of the *trans* form is thermally quite stable. In addition, the abrupt weight-loss is a typical sign for one component system, as is also shown by the mass spectrum (Fig. 3). Furthermore, it is important to note that Na-free B-PAT of the *trans* form can be sublimated under high vacuum, showing an extremely high thermal stability. This is an usual characteristic that is not found in ordinary bisazo compounds.

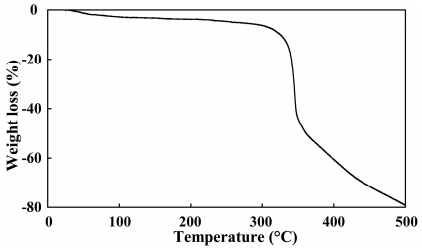

Fig. 12 Thermogravimetric analysis of Na-free B-PAT of the trans form.

3.2.3. Solvent fastness

As stated in introduction, the mixture of Na-containing B-PAT of the *cis* form and M-PAT is highly resistant to light irradiation and heat, but is rather poor in solvent fastness. On the contrary, Na-free B-PAT of the *trans* form is found to possess much higher solvent fastness in addition to the light and heat stability.

The solubility of Na-free B-PAT in DMA and NMP is 1 g/l and 5 g/l, respectively. This is nearly equivalent to that of Pigment Red 255 (*i.e.* diketopyrrolopyrrole derivative). On the other hand, Na-containing B-PAT exhibits a solubility of about 25 g/l in NMP.

4. Conclusions

Electronic characterization together with light-, heat-, solvent fastness has been carried out on Na-free B-PAT of the *trans* form, using the mixture of originally synthesized B-PAT (*i.e.* mixture of Na-containing B-PAT of *cis* form and M-PAT). The conclusions can be summarized as follows.

1. There are two optical transitions in the visible region according to the MO calculations: one is the transition of 450 nm with an oscillator strength of 1.08 composed of the transitions of HOMO to LUMO+1, HOMO to LUMO+2, and HOMO-1 to LUMO, and the other is the transition of 403 nm with an oscillator strength of 0.34 consisting of the transitions of HOMO-1 to LUMO and HOMO to LUMO+1.

2. The solution spectrum of Na-free B-PAT of *trans* form in NMP exhibits a vivid yellow as characterized by a broad band between 380 and 500 nm. The absorption maximum is assigned to the 0-1 vibronic transition, assuming that the main component as described above prevails. No significant difference is recognized between the spectra in solution and solid state as far as the spectral region is concerned. However, the solid state spectra are slightly broader than that in solution, and the absorption maximum is located slightly at shorter wavelengths.

3. Na-free B-PAT of the *trans* form is resistant to light-, heat-, and solvent. Elimination of the Na atom from Na-containing B-PAT of the *cis* form is the key to the single component system of the *trans* form which yields a yellow pigment that possesses good pigmentary characteristics.

References

[1] H. Zollinger: Color Chemistry, Wiley-VCH (2003).

[2] Y. Nagata and K. Tateishi: Jpn Patent, 2009-73978 A, (2009).

[3] H. Shibata and J. Mizuguchi: Four crystal-structures derived from a yellow pyrazolyl azo pigment, Proceedings of NIP26 (2010).

[4] H. Shibata and J. Mizuguchi: (2,6-Bis{5-amino-3-*tert*- butyl-4-[(3-methyl-1,2,4-thiadiazol-5-yl)diazenyl]-1*H*- pyrazol-1-yl}-4-oxo-1,4-dihydro-1,3,5-triazin-1-ido) methanol(phenol)sodium phenol tetrasolvate, Acta Cryst. E**66**, m463-m464 (2010).

[5] H. Shibata and J. Mizuguchi: (2,6-Bis{5-amino-3-*tert*- butyl-4-[(3-methyl-1,2,4-thiadiazol-5-yl)diazenyl]-1*H*- pyrazol-1-yl}-4-oxo-1,4-dihydro-1,3,5-triazin-1-ido) *N*-methyl-2-pyrrolidone(water)sodium *N*-methyl-2-pyrrolidone, accepted for publication in X-ray structure analysis online (2010),.

[6] H. Shibata and J. Mizuguchi: 6-{5-amino-3-*tert*-butyl- 4-[(*E*)-(3-methyl-1,2,4-thiadiazol-5-yl)diazenyl]-1H-pyrazol-1-yl}-1,3,5-triazine-2,4-(1*H*,3*H*)-dione-1-methylpyrrolidin-2-one-water, Acta Cryst. E**66**, o944-o945 (2010).

Author Biography

Hiroki Shibata received his Bachelor of Engineering in 2008 and his Master of Engineering in 2010, both from Yokohama National University. He is currently in the doctor's course for applied physics at the same university. His research interest includes structure analysis of azo pigments and their electronic applications.